# Organogel Actuators Based on Redox-Responsive Foldamers: Amplification of Molecular Machine's Motion to Macroscopic Scale

*Taichi Ikeda**

Research Center for Functional Materials, National Institute for Materials Science, 1-1 Namiki Tsukuba, Ibaraki, 305-0044, Japan. E-mail: IKEDA.Taichi@nims.go.jp

ABSTRACT

The amplification of nano-scale motions of artificial molecular machines to the macroscopic level is a major challenge. In this study, a redox-responsive donor–acceptor (DA)-type foldamer, in which tetrathiafulvalene (TTF) and viologen units are alternatively connected, was installed in an organogel network as a "working unit" to induce actuation. The ion gels were successfully synthesized via thermal azide–alkyne cycloaddition reaction between azide-functionalized foldamer and the tetra-alkyne-ester crosslinker in an ionic liquid. The reaction efficiency of crosslink was estimated from the stress-elongation curve. It was confirmed that the foldamers kept their electrochemical activity in the gel. Redox-responsive actuation of the gel was confirmed in a 0.1 M tetrabutylammonium·$PF_6$ acetonitrile solution. Through chemical oxidation, the characteristic length of the gel could be increased up to 125% of its initial length, indicating the volume of the gel could be increased to 195%. Reversible gel size changes in response to the redox reactions were confirmed. The change in the gel size was induced by equilibrium shift of the foldamer conformation between the folded state and extended state. The actuation force during the reduction of the partially-oxidized gel was ca. 3.4 kPa, indicating that the gel can generate 35 gf $cm^{-2}$. This actuation force proves a great potential for the redox-responsive foldamers to act as a molecular machine for realizing macroscopic actuation.

Keywords: Molecular machines • Foldamers • Stimuli-responsive materials • Gels • Actuators

## 1. Introduction

The polymer-based artificial muscles are attractive because it can realize lighter-weight, lower energy consumption, and more silent actuator than the mechanical actuators.[1–5] The stimuli-responsive gel can change its volume by altering the swelling property of the gel network or the crosslinking density by external stimuli.[6,7] The systems of the conventional gel actuators are completely different from those in nature. In biological systems, the skeletal muscles can work on the macroscopic scale via the amplification of small motions generated by the basic "working units" (actin and myosin filaments) that can convert chemical energy into mechanical work.[8,9] It is a great challenge to realize similar system to skeletal muscle using artificial molecular machines.[10–14] The examples of the actuators assembled from the artificial molecular machines that can exhibit macroscopic deformation are limited. J. F. Stoddart *et al.* succeeded to bend the atomic force microscopy (AFM) cantilever by the actuation forces of the rotaxane-based molecular machines assembled on the AFM cantilever surface.[15,16] This demonstration was detectable from the change in the laser light reflection angle, indicating the deformation of the AFM cantilever was too small to be detected by the naked eye. Recently, some groups reported macroscopic deformation of the gel actuator consisting of the molecular machines as the working units. N. Giuseppone *et al.* reported that mechanically active hydrogels comprised of [*c*2] daisy chain rotaxanes.[17] Furthermore, their group succeeded in achieving actuation based on the braiding of the polymer chains via the mechanical rotation of the light-driven molecular motor.[18,19] A. Harada *et al.* also reported on the hydrogel actuator based on [*c*2] daisy chain rotaxanes.[20]

In this study, the foldamer was selected as a working unit because its polymeric structure has good compatibility with the polymer-gel actuators (**Figure** 1).[21–24] J. C. Barnes *et al*. reported on the redox-responsive actuation of the hydrogel consisting of linearly connected viologen

polymers.[25] When the viologen unit was reduced to the radical cation state, the conformation of the viologen polymer was found to alter from the extended state to the folded state due to the radical-based self-assembly of the viologen units.[25,26] Since a volume change of the gel occurred during the reduction process, the actuator could work only under *anaerobic conditions* inside a $N_2$-filled glovebox.[25,27,28] This is a serious drawback for practical application.

Based on this perspective, we aim to develop the foldamer-based gel actuators that also function in *aerobic conditions* (under oxidative condition in air). The donor–acceptor (DA)-type foldamer is a promising candidate as a working unit because its conformation change between the folded state and extended state is electrochemically controllable.[29–32] In our previous study, the DA-type foldamers consisting of tetrathiafulvalene (TTF, electron donor) and viologen (electron acceptor) units were successfully synthesized, and their thermal and electrochemical properties were characterized.[33] Here, the terminal group of the foldamer is changed from the methoxy group to the azide group for the chemical crosslink reaction. The ion gels were prepared via copper-free azide–alkyne cycloaddition (AAC) reaction[34–37] between the azide-functionalized foldamer and the tetra-alkyne-ester crosslinker in an ionic liquid (**Figure** 1). Due to the negligible vapor pressure of the ionic liquid, a gel film with a well-defined polymer concentration and thickness was obtained under vacuum conditions, which enabled mechanical characterization and actuation force measurements using a tensile testing machine. The gel size change in response to the redox-reaction was investigated. The actuation force in the reduction process of the partially oxidized gel was measured using a tensile machine in the solution.

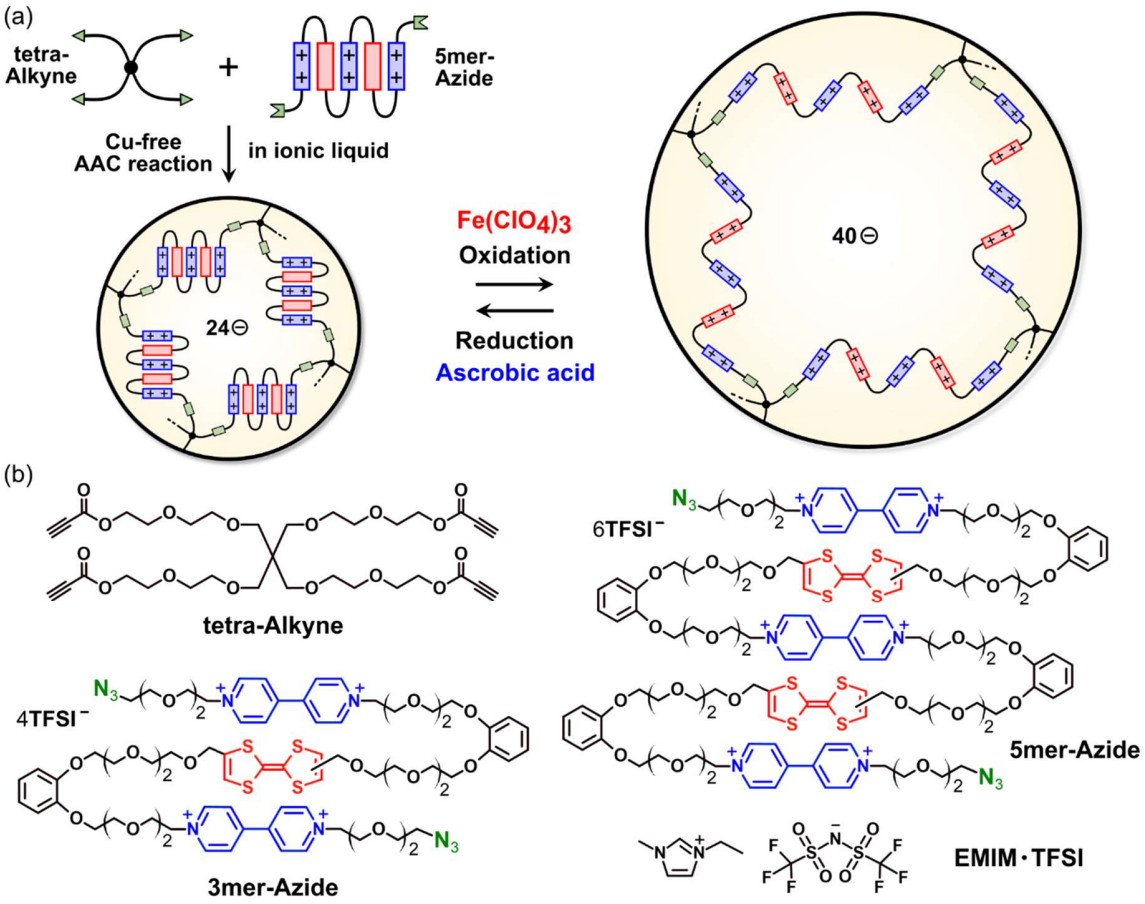


**Figure 1**. (a) Schematic illustration of gel actuator preparation through copper-free azide-alkyne cycloaddition reaction between **tetra-Alkyne** crosslinker and **5mer-Azide** redox-responsive foldamer. (b) Chemical structures of **tetra-Alkyne**, **3mer-azide**, **5mer-Azide** and ionic liquid **EMIM·TFSI**.

## 2. Experimental Section

**2.1. Ion Gel Preparation: 3mer-Azide** (67.5 mg, Azide group: $5.0 \times 10^{-5}$ mol) and 1-ethyl-3-methylimidazolium bis(trifluoromethanesulfonyl)imide (**EMIM·TFSI**) (114.4 mg) were dissolved in acetone (1.0 mL). **tetra-Alkyne** (17.5 mg) was dissolved in 1.0 mL acetone. The solution of **tetra-Alkyne** (0.50 ml, Alkyne group: $5.0 \times 10^{-5}$ mol) was added to the **3mer-Azide**

solution. The acetone was removed by evaporation under reduced pressure at 20 °C. The ionic liquid solution was cured between orthogonally arranged two glass slides (2.5 cm × 7.5 cm) at 70 °C for 24 h under reduced pressure using a vacuum oven (ETTAS AVO-250V). The gap between two glass slides was controlled with a spacer (Thickness: 0.15–0.25 mm). The ion gel was peeled off from the glass slides, cut to an appropriate size and shape and used for instrumental analysis. The thickness of each sample gel was checked with an optical microscope. For electrochemical analysis, the gel was prepared on glassy carbon electrode at 70 °C for 24 h under reduced pressure.

**2.2. Chemical Redox Reaction of Organogel**: The ion gel was immersed in 0.1 M tetrabutylammonium hexafluorophosphate (TBA·$PF_6$) acetonitrile solution (4 mL) for 5 min in three times for exchanging the swelling solution. For chemical oxidation, the organogel was immersed in the 0.1 M TBA·$PF_6$ acetonitrile solution (4 mL), then 50 mM $Fe(ClO_4)_3$ acetonitrile solution (1 mL) was added to the solution. After an appropriate reaction time, the organogel was picked up from the solution and immersed in the 0.1 M TBA·$PF_6$ acetonitrile solution (4 mL) for 2 min in three times for removing $Fe(ClO_4)_3$ and for reaching the equilibrium under the same environment as the initial condition. The characteristic length of the gel, which was defined as the sum of the lengths of two diagonals of the rectangle-shaped gel, was measured. The ascorbic acid (176 mg) was dissolved in 1 mL water then diluted with 9 mL acetonitrile for preparing 100 mM ascorbic acid solution. For chemical reduction, the organogel was immersed in the 0.1 M TBA·$PF_6$ acetonitrile solution (4 mL), then 100 mM ascorbic acid solution (1 mL) was added to the solution. After an appropriate reaction time, the size of the organogel was measured through the same procedure as that for chemical oxidation.

**2.3. Actuation force measurement**: The ion gel was immersed in 0.1 M TBA·$PF_6$ acetonitrile solution (4 mL) for 5 min in three times for exchanging the swelling solution. For chemical oxidation, the organogel was immersed in the 0.1 M TBA·$PF_6$ acetonitrile solution (4 mL), then 50 mM $Fe(ClO_4)_3$ acetonitrile solution (1 mL) was added to the solution. After 4 min, the organogel was picked up from the solution and immersed in the 0.1 M TBA·$PF_6$ acetonitrile solution (4 mL) for 2 min in three times for removing $Fe(ClO_4)_3$ and for reaching the equilibrium under the same environment as the initial condition. The gel was set to an immersion type tensile tester (Stency, AcroEdge). The gel sample was immersed in the 0.1 M TBA·$PF_6$ acetonitrile solution (80 mL) using a solution bath. After applying 5% strain on the organogel sample, 100 mM ascorbic acid solution (20 mL) was added to the solution bath. The actuation force of the sample in response to the chemical reduction of the partially-oxidized gel was monitored with keeping a constant sample length until the color of the gel turned to green.

## 3. Results and Discussion

**3.1. Synthesis and gel preparation.** Two types of the foldamers containing different number of DA units (**3mer-Azide**, and **5mer-Azide**), and the crosslinker **tetra-Alkyne** were synthesized according to **Scheme** S1. The chemical structure of all compounds was confirmed via $^{1}H$- and $^{13}C$-NMR spectroscopy as well as high-resolution electrospray ionization mass spectrometry (HR-ESI-MS) **(Figure**s S1–S7). The ion gels were prepared via copper-free AAC reaction between the azide-functionalized foldamer and the tetra-alkyne-ester crosslinker in an ionic liquid **EMIM·TFSI**. Utilization of an ionic liquid gave some advantages: (i) Gels can be prepared under vacuum condition, which contributes to remove the gas bubbles arising from the solvent

evaporation. (ii) One can avoid the volume and polymer concentration changes by solvent evaporation. (iii) One can prepare the gel with a well-defined shape and thickness, which facilitates mechanical characterization of the gel using a tensile machine. The ion gels prepared from **3mer-azide** and **5mer-azide** refer to 3mer and 5mer gels, respectively. After the reaction at 70°C for 24h, the mechanically-tough green-color ion gel was obtained (see the supplementally video). The polymer concentration of the gel was set to be 40 wt%. When the polymer concentration was set to be 30%, the gels was mechanically too weak to peel off from the glass slide.

Although the TTF and the viologen have no visible-light absorption over 500 nm wavelength, the foldamer shows the absorption peak around 750 nm wavelength. This peak arises from the charge transfer (CT) between the donor (TTF) and the acceptor (viologen) units.[32,38,39] The CT absorption band intensity of the ion gel was measured by UV-Vis spectrum measurement. The concentration of the 3mer unit in the ion gel was calculated to be 0.19 M. From the thickness of the gel (0.14 mm) and absorbance at 750 nm (1.666), the molar extinction coefficient ($\varepsilon$) of the CT band was calculated to be 620 $M^{-1}$ $cm^{-1}$. In the solution state, the $\varepsilon$ value of the model 3mer at 750 nm was 490 $M^{-1}$ $cm^{-1}$ (Concentration: $5.0 \times 10^{-4}$ M in **EMIM·TFSI**, 20°C).[33] This result suggests larger CT band intensity in the gel than that in the solution. In the case of the gel, the foldamer units were immobilized in the gel network and these were placed nearby. Therefore, it is considered that CT between the DA units belonging to the different foldamer chains became possible. This issue will be discussed later again.

**Figure** S8 shows IR spectra of the starting materials and the ion gel. The samples of the **tetra-Alkyne** (**Figure** S8b) and **5mer-azide** (**Figure** S8c) were found to exhibit characteristic IR peaks corresponding to C≡C stretching (open circles) and $N_3$ stretching (filled circles), respectively. These peaks were disappeared in the spectra of the ion gel (**Figure** S8d). Strong C=O stretching

peak was observed for **tetra-Alkyne** (**Figure** S8b, open triangle). That peak in the 5mer ion gel was small, but detectable in the IR spectra (**Figure** S8d, open triangle). In order to obtain more intensive peaks of the polymer network, the solvent of the gel was removed through exchanging the solvent from **EMIM·TFSI** to dichloromethane followed by the evaporation of the solvent under reduced pressure. The IR spectrum of the 5mer gel after removing the ionic liquid was shown in **Figure** S8e. The spectrum gave no C≡C stretching nor $N_3$ stretching peaks but intensive C=O stretching peak.

**3.2. Mechanical property of foldamer ion gel.** The mechanical properties were characterized with a tensile machine. The elastic modulus ($G_e$) was obtained from the fitting for the initial stage of the stress-elongation curve by the equation (1).[40]

$$\sigma_{stress} = G_e(\lambda - \lambda^{-2}) \qquad (1)$$

where $\sigma_{stress}$ and $\lambda$ are stress and elongation, respectively. The values of $G_e$, fracture stress ($\sigma_f$), and fracture strain ($\varepsilon_f$) are summarized in **Table** 1. The foldamer ion gel exhibited a typical S-shaped stress–strain curve (**Figure** 2).[40–42] The $G_e$ value of the 3mer ion gel was larger than that of the 5mer ion gel. This result can be attributed to the higher crosslink density of the 3mer ion gel. The reaction efficiency of crosslink ($p$) can be estimated from the value of $G_e$ (The $p$ value of 1.0 means the completion of AAC reaction in 100% yield, see the Supporting Information).[43,44] The calculated $p$ value of the 3mer and 5mer ion gels were 0.70 and 0.71, respectively, indicating that the reaction efficiencies were similar in the two cases. Comparing these values with the reported value for tetra-PEG ion gel synthesis using copper-free AAC reaction ($p$ = 0.90),[37] the reaction efficiency in this study was low. Complete disappearance of the C≡C stretching and $N_3$

stretching IR peaks (**Figure** S8e) indicates that the copper-free AAC reaction proceeded almost perfectly. Therefore, it is considered that short ethylene oxide chains of the **tetra-Alkyne** and the folded conformation of the foldamer would facilitate to form the loop structure, in which both terminal azide groups of the foldamer react with the same **tetra-Alkyne** unit. The larger $\varepsilon_f$ value of the 5mer gel than the 3mer gel reflects higher capability of the end-to-end distance change of the 5mer foldamer due to the compact conformation in the initial state by polymer folding.

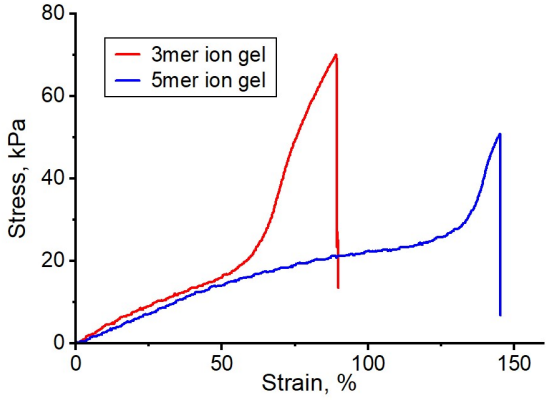


**Figure** 2. Stress-strain curves of 3mer (red) and 5mer ion gels (blue).

**Table** 1. Mechanical properties of foldamer ion gels (average ± standard deviation, $n = 3$)

| Sample | $G_e$ [a] kPa | $\sigma_f$ [b] kPa | $\varepsilon_f$ [c] % |
|---|---|---|---|
| 3mer ion gel | 19 ± 3 | 55 ± 13 | 82 ± 11 |
| 5mer ion gel | 14 ± 2 | 44 ± 15 | 142 ± 6 |

[a] Elastic modulus, [b] Fracture stress, [c] Fracture strain

**3.3. Electrochemical property of foldamer ion gel.** For the electrochemical analysis, the ion gels were prepared on the glassy carbon electrodes and their electrochemical properties were analyzed by cyclic voltammetry (**Figure** S10). **Figure** 3a shows cyclic voltammograms of the 3mer and 5mer ion gels. It was confirmed that the foldamer maintained its electrochemical activity after gelation. The peaks originating from the redox reactions of the TTF and the viologen units were detectable in the positive and negative potential regions, respectively.[45–47] **Table** 2 summarizes the half-wave potential of each redox reaction. It was not feasible to determine the second reduction potential of the viologen unit because of a solubility issue that pollutes the electrode surface with the aggregation of the gel network.[33] The CV curve in **Figure** S12 indicates that the working electrode was not able to detect the current flow below −0.85 V because of the surface pollution. The anodic peak current of the TTF first oxidation reaction varied linearly with the square root of the scan rate (**Figure** 3b). This result indicates that the redox process is diffusion controlled, and the electron hopping between the TTF units inside the gel occurs.[48] However, it was nonviable to oxidize the whole part of the ion gels with 0.2 mm thickness presumably due to the limitation of electrochemical reaction imposed by the electron hopping.

**Table** 2. Half-wave potentials (vs $Ag/Ag^+$) of foldamer ion gels[a]

| Sample | $E_{-1}$[b] V | $E_{+1}$[c] V | $E_{+2}$[d] V |
|---|---|---|---|
| 3mer ion gel | −0.36 | +0.39 | +0.79 |
| 5mer ion gel | −0.35 | +0.38 | +0.80 |

[a] Nitrogen purged EMIM·TFSI, Scan rate: 200 mV $s^{-1}$. [b] First reduction potential (Viologen radical cation/Viologen dication), [c] First oxidation potential (TTF/TTF radical cation), [d] Second oxidation potential (TTF radical cation/TTF dication).

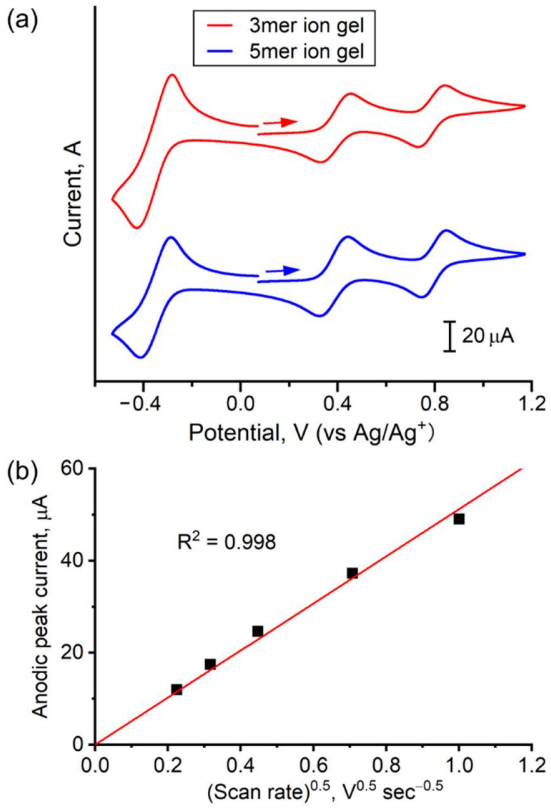


**Figure** 3. (a) Cyclic voltammogram of 3mer ion gel (red) and 5mer ion gel (blue) on a glassy carbon electrode (0.07 $cm^2$). Scan rate: 200 mV $s^{-1}$. Electrolyte: nitrogen purged EMIM·TFSI. Counter electrode: Pt wire. Reference electrode: $Ag/Ag^+$. (b) Scan rate dependency of anodic peak current of the first oxidation peak of 3mer ion gel. Fitting line was depicted in red.

### 3.4. Chemical actuation of foldamer organogels

Prior to the chemical oxidation experiment of the foldamer gel, the swelling solution of the gel was substituted; the ionic liquid was replaced with an organic solvent (acetonitrile) due to the solubility issue with the chemical oxidant [$Fe(ClO_4)_3$] and reductant (ascorbic acid). In order to

suppress the gel network expansion caused by osmic pressure,[49] 0.1 M TBA·$PF_6$ acetonitrile solution was used as the swelling solution.

**Figure** 4a shows the change in the UV–Vis spectrum for the 3mer organogel in response to the chemical oxidation. As mentioned above, the 3mer gel shows absorption peak around 750 nm wavelength due to CT interaction [**Figure** 4a (i)]. At partially oxidized state, not only the peak of the TTF radical cation at the wavelength of 600 nm, but also that of the TTF radical dimer was observed at 770 nm [**Figure** 4a (ii)].[50–52] In case of the model 3mer in solution, the TTF radical dimer formation was not observed because the model 3mer molecule had only one TTF unit and each molecule was isolated in the solution.[33] This result suggests that the TTF units belonging to the different foldamer chains can form radical dimers in the gel. This result is consistent with the finding of the larger CT band intensity in the gel compared with that observed in the solution as discussed above. When the TTF unit was completely oxidized, no peak was observed in the range of 500–900 nm wavelength, indicating the formation of the TTF dication [**Figure** 4a (iii)].[33,46]

**Figure** 4b shows the change in the gel size during chemical oxidation. Since the size of the gel is sensitive to the solution condition, the chemical oxidant (or reductant) was removed by immersing the organogel in the stock solution of 0.1 M TBA·$PF_6$ acetonitrile solution before measuring the characteristic length of the gel at each time. The characteristic length of the gel increased monotonically with time. After complete oxidation, the characteristic lengths of the 3mer and 5mer organogels increased to 119 ± 2% and 125 ± 1% (average ± standard deviation, $n$ = 5) of their initial states, respectively. This change in dimension was attributable to the equilibrium shift of the foldamer from the folded state to the extended state due to the electrostatic repulsive force between the TTF dication and viologen units.[33] It is considered that the larger deformation of the 5mer organogel than the 3mer organogel reflects the larger change in the end-to-end distance of

the foldamer by the conformation change (folded state and extended state). The change in the characteristic length of the gel in response to the conformation change of the foldamer looks to be smaller than the expectation from the image shown in **Figure** 1a. This is because the foldamer in this study has low degree of polymer folding (<0.5) in its initial state (neutral TTF at room temperature).[33] When the oxidized organogel was reduced by ascorbic acid, the gel shrank to its original size. The repeatability of the gel size change in response to the redox reaction was confirmed (**Figure** 4c).

The actuation force in the reduction process of the oxidized organogel in the solution was measured using an immersion type tensile tester (**Figure** 4d). The partially-oxidized organogel was utilized for actuation force measurement, because the completely oxidized organogel lost the mechanical toughness and it was easily broken during the measurement. The actuation forces of the 3mer and 5mer organogel were found to be 3.4 ± 1.3 and 3.2 ± 0.8 kPa (average ± standard deviation, $n$ = 3), respectively. When the gel was completely reduced, the color of the gel turned to green (inset in **Figure** 4d), indicating the CT interaction between the DA units recovered. Since this experiment was done under aerobic condition (oxidative condition in air), the reduction of the viologen unit was not observed.

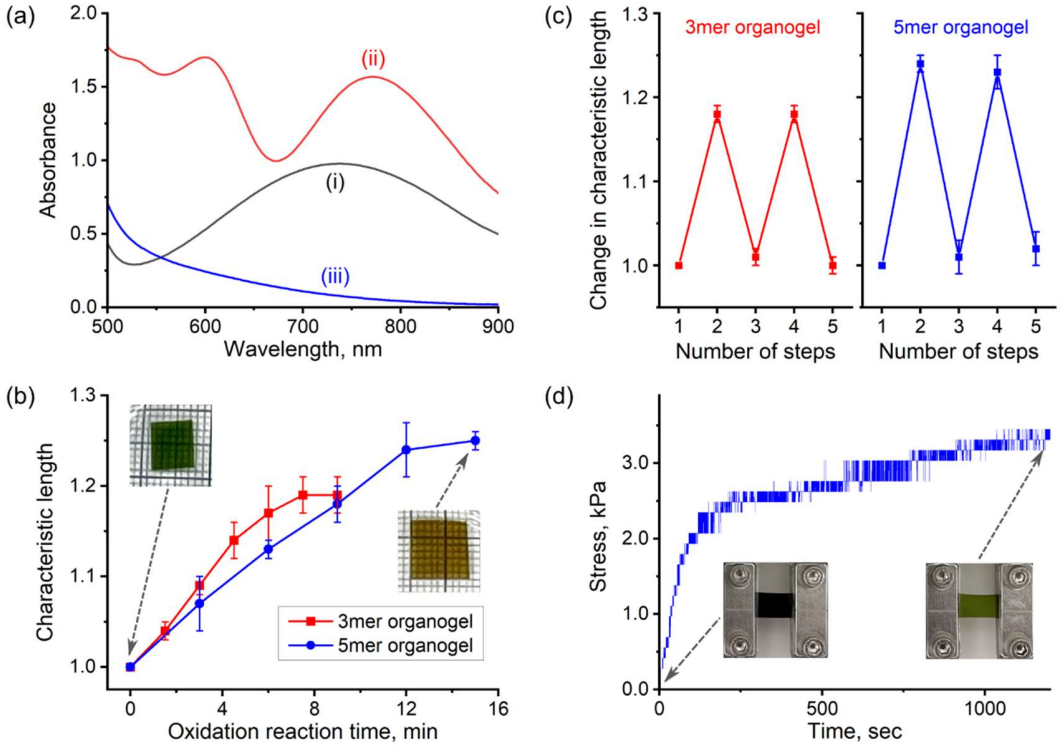


**Figure** 4. (a) Absorption spectra of 3mer organogel at different oxidation states. (i) Initial state. (ii) Partially oxidized state. (iii) Completely oxidized state. (b) Change in characteristic length in chemical oxidation process for 3mer organogel (red color) and 5mer organogel (blue color) (average ± standard deviation, $n$ = 5). Inset shows photograph of 5mer organogel at initial state (upper left) and at completely oxidized state (right). (c) Cyclability test of gel size change. Odd and even number steps correspond to the neutral and dication states of the TTF unit in the foldamer gel (average ± standard deviation, $n$ = 5). (d) Actuation force measurement in reduction process of partially oxidized 5mer organogel in the solution (gel thickness 0.27 mm, width 5.4 mm). Inset shows photograph of 5mer organogel before applying 5% strain (bottom left) and after chemical reduction (bottom right). The change in the stress was plotted after adding the ascorbic acid solution.

## 4. Conclusion

The ion gels consisting of the DA-type redox-responsive foldamers were successfully prepared via copper-free AAC reaction between azide-functionalized foldamer and tetra-alkyne crosslinker in the ionic liquid. The reaction efficiency of crosslink was estimated to be *ca*. 70% from the elastic modulus of the ion gel. Compared with the model foldamer in the solution, the observations of a larger CT band intensity and the TTF radical dimer formation in the 3mer gel suggest that the DA units belonging to the different foldamer chains can interact with each other in the gel network. Through chemical oxidation, the characteristic length of the organogel increased up to 125%, indicating the volume of the gel could be increased to 195%. The actuation force of 3.4 kPa in the reduction process of the partially-oxidized organogel corresponds to 35 gf $cm^{-2}$. It should be noted that larger actuation force can be expected if the degree of polymer folding in the initial state, the reaction efficiency of crosslink, and the mechanical toughness of the completely oxidized organogel could be improved. Therefore, it was concluded that the DA-type foldamer is a promising molecular machine for realizing macroscopic deformations.

.

ASSOCIATED CONTENT

**Supporting Information.** The Supporting Information is available free of charge via the Internet at http://pubs.acs.org.

Materials and methods, Synthesis, $^{1}H$ and $^{13}C$ NMR spectra, HR-ESI-MS, IR, Video of stretching the ion gel sample, Calculation of reaction efficiency from elastic modulus, Electrochemical measurement setup, Cyclic voltammogram of foldamer gel in scan range from 0.0 V to −1.0 V (PDF).

## AUTHOR INFORMATION


### Corresponding Author

* E-mail: IKEDA.Taichi@nims.go.jp


### Notes

The author declares no competing financial interest.

## ACKNOWLEDGMENT


The author gratefully acknowledges financial support for this work by M-Cube projects in National Institute for Materials Science (NIMS).


## REFERENCES


(1) Chen, D.; Pei, Q. B. Electronic Muscles and Skins: A Review of Soft Sensors and Actuators. *Chem. Rev.* **2017**, *117,* 11239−11268.

(2) Mirvakili, S. M.; Hunter, I. W. Artificial Muscles: Mechanisms, Applications, and Challenges. *Adv. Mater.* **2018**, *30*, 1704407.

(3) El-Atab, N.; Mishra, R. B.; Al-Modaf, F.; Joharji, L.; Alsharif, A. A.; Alamoudi, H.; Diaz, M.; Qaiser, N.; Hussain, M. M. Soft Actuators for Soft Robotic Applications: A Review. *Adv. Intell. Syst.* **2020**, *2*, 2000128.

(4) McCracken, J. M.; Donovan, B. R.; White, T. J. Materials as Machines. *Adv. Mater.* **2020**, *32*, 1906564.

(5) Xiong, J. Q.; Chen, J.; Lee, P. S. Functional Fibers and Fabrics for Soft Robotics, Wearables, and Human-Robot Interface. *Adv. Mater.* **2021**, *33*, 2002640.

(6) Koetting, M. C.; Peters, J. T.; Steichen, S. D.; Peppas, N. A. Stimulus-Responsive Hydrogels: Theory, Modern Advances, and Applications. *Mater. Sci. Eng. R Rep.* **2015**, *93,* 1−49.

(7) Mondal, S.; Das, S.; Nandi, A. K. A Review on Recent Advances in Polymer and Peptide Hydrogels. *Soft Matter* **2020**, *16,* 1404−1454.

(8) Frontera, W. R.; Ochala, J. Skeletal Muscle: A Brief Review of Structure and Function. *Calcif. Tissue Int.* **2015**, *96,* 183−195.

(9) Mukund, K.; Subramaniam, S. Skeletal Muscle: A Review of Molecular Structure and Function, in Health and Disease. *Wiley Interdiscip. Rev. Syst. Biol. Med.* **2020**, *12*, e1462.

(10) Bruns, C. J.; Stoddart, J. F. Rotaxane-Based Molecular Muscles. *Acc. Chem. Res.* **2014**, *47,* 2186−2199.

(11) Niess, F.; Duplan, V.; Sauvage, J. P. Molecular Muscles: From Species in Solution to Materials and Devices. *Chem. Lett.* **2014**, *43,* 964−974.

(12) Erbas-Cakmak, S.; Leigh, D. A.; McTernan, C. T.; Nussbaumer, A. L. Artificial Molecular Machines. *Chem. Rev.* **2015**, *115,* 10081−10206.

(13) Dattler, D.; Fuks, G.; Heiser, J.; Moulin, E.; Perrot, A.; Yao, X. Y.; Giuseppone, N. Design of Collective Motions from Synthetic Molecular Switches, Rotors, and Motors. *Chem. Rev.* **2020**, *120,* 310−433.

(14) Perrot, A.; Moulin, E.; Giuseppone, N. Extraction of Mechanical Work from Stimuli-Responsive Molecular Systems and Materials. *Trends Chem.* **2021**, *3,* 926−942.

(15) Liu, Y.; Flood, A. H.; Bonvallett, P. A.; Vignon, S. A.; Northrop, B. H.; Tseng, H. R.; Jeppesen, J. O.; Huang, T. J.; Brough, B.; Baller, M.; Magonov, S.; Solares, S. D.; Goddard, W. A.; Ho, C. M.; Stoddart, J. F. Linear Artificial Molecular Muscles. *J. Am. Chem. Soc.* **2005**, *127,* 9745−9759.

(16) Juluri, B. K.; Kumar, A. S.; Liu, Y.; Ye, T.; Yang, Y. W.; Flood, A. H.; Fang, L.; Stoddart, J. F.; Weiss, P. S.; Huang, T. J. A Mechanical Actuator Driven Electrochemically by Artificial Molecular Muscles. *ACS Nano* **2009**, *3,* 291−300.

(17) Goujon, A.; Lang, T.; Mariani, G.; Moulin, E.; Fuks, G.; Raya, J.; Buhler, E.; Giuseppone, N. Bistable [*c*2] Daisy Chain Rotaxanes as Reversible Muscle-Like Actuators in Mechanically Active Gels. *J. Am. Chem. Soc.* **2017**, *139,* 14825−14828.

(18) Li, Q.; Fuks, G.; Moulin, E.; Maaloum, M.; Rawiso, M.; Kulic, I.; Foy, J. T.; Giuseppone, N. Macroscopic Contraction of a Gel Induced by the Integrated Motion of Light-Driven Molecular Motors. *Nat. Nanotechnol.* **2015**, *10,* 161−165.

(19) Foy, J.; Li, Q.; Goujon, A.; Collard, J. R.; Fuks, G.; Moulin, E.; Schiffman, O.; Dattlier, D.; Funeriu, D.; Giuseppone, N. Dual-Light Control of Nanomachines That Integrate Motor and Modulator Subunits. *Nat. Nanotechnol.* **2017**, *12,* 540−545.

(20) Iwaso, K.; Takashima, Y.; Harada, A. Fast Response Dry-Type Artificial Molecular Muscles with [c2] Daisy Chains. *Nat. Chem.* **2016**, *8,* 626−633.

(21) Khan, A.; Hecht, S. Towards Photocontrol over the Helix-Coil Transition in Foldamers: Synthesis and Photoresponsive Behavior of Azobenzene-Core Amphiphilic Oligo(*meta*-phenylene ethynylene)s. *Chem. Eur. J.* **2006**, *12,* 4764−4774.

(22) Cai, W.; Wang, G. T.; Du, P.; Wang, R. X.; Jiang, X. K.; Li, Z. T. Foldamer Organogels: A Circular Dichroism Study of Glucose-Mediated Dynamic Helicity Induction and Amplification. *J. Am. Chem. Soc.* **2008**, *130,* 13450−13459.

(23) Shibata, M.; Tanaka, S.; Ikeda, T.; Shinkai, S.; Kaneko, K.; Ogi, S.; Takeuchi, M. Stimuli-Responsive Folding and Unfolding of a Polymer Bearing Multiple Cerium(IV) Bis(porphyrinate) Joints: Mechano-Imitation of the Action of a Folding Ruler. *Angew. Chem. Int. Ed.* **2013**, *52,* 397−400.

(24) Rodriguez, R.; Suarez-Picado, E.; Quinoa, E.; Riguera, R.; Freire, F. A Stimuli-Responsive Macromolecular Gear: Interlocking Dynamic Helical Polymers with Foldamers. *Angew. Chem. Int. Ed.* **2020**, *59,* 8616−8622.

(25) Greene, A. F.; Danielson, M. K.; Delawder, A. O.; Liles, K. P.; Li, X. S.; Natraj, A.; Wellen, A.; Barnes, J. C. Redox-Responsive Artificial Molecular Muscles: Reversible Radical-Based Self-Assembly for Actuating Hydrogels. *Chem. Mater.* **2017**, *29,* 9498−9508.

(26) Wang, Y. P.; Frasconi, M.; Liu, W. G.; Liu, Z. C.; Sarjeant, A. A.; Nassar, M. S.; Botros, Y. Y.; Goddard, W. A.; Stoddart, J. F. Folding of Oligoviologens Induced by Radical-Radical Interactions. *J. Am. Chem. Soc.* **2015**, *137,* 876−885.

(27) Amir, F.; Liles, K. P.; Delawder, A. O.; Colley, N. D.; Palmquist, M. S.; Linder, H. R.; Sell, S. A.; Barnes, J. C. Reversible Hydrogel Photopatterning: Spatial and Temporal Control over Gel Mechanical Properties Using Visible Light Photoredox Catalysis. *ACS Appl. Mater. Interfaces* **2019**, *11,* 24627−24638.

(28) Danielson, M. K.; Chen, J.; Vaclavek, A. K.; Colley, N. D.; Alli, A.-H.; Loomis, R. A.; Barnes, J. C. Photoinduced Electron Transfer and Changes in Surface Free Energy in Polythiophene-Polyviologen Bilayered Thin Films. *ACS Polym. Au* **2022**, *2,* 118−128.*I*

(29) Lokey, R. S.; Iverson, B. L. Synthetic Molecules That Fold into a Pleated Secondary Structure in Solution. *Nature* **1995**, *375,* 303−305.

(30) Ghosh, S.; Ramakrishnan, S. Aromatic Donor-Acceptor Charge-Transfer and Metal-Ion-Complexation-Assisted Folding of a Synthetic Polymer. *Angew. Chem. Int. Ed.* **2004**, *43,* 3264−3268.

(31) Bruns, C. J.; Stoddart, J. F. Mechanically Interlaced and Interlocked Donor-Acceptor Foldamers. In *Hierarchical Macromolecular Structures: 60 Years after the Staudinger Nobel Prize I, Vol. 261* (Ed.: V. Percec); Springer, 2013; pp. 271−294.

(32) Chen, L.; Wang, H.; Zhang, D. W.; Zhou, Y. M.; Li, Z. T. Quadruple Switching of Pleated Foldamers of Tetrathiafulvalene-Bipyridinium Alternating Dynamic Covalent Polymers. *Angew. Chem. Int. Ed.* **2015**, *54,* 4028−4031.

(33) Ikeda, T.; Nakanishi, W. Thermal and Redox Properties of Donor-Acceptor Foldamers Consisting of Tetrathiafulvalene and Viologen. *Mater. Today Chem.* **2022**, *24*, 100863.

(34) Kolb, H. C.; Finn, M. G.; Sharpless, K. B. Click Chemistry: Diverse Chemical Function from a Few Good Reactions. *Angew. Chem. Int. Ed.* **2001**, *40,* 2004−2021.

(35) Gorman, I. E.; Willer, R. L.; Kemp, L. K.; Storey, R. F. Development of a Triazole-Cure Resin System for Composites: Evaluation of Alkyne Curatives. *Polymer* **2012**, *53,* 2548−2558.

(36) Ikeda, T. Copper-Free Synthesis of Glycidyl Triazolyl Polymers. *Macromol. Chem. Phys.* **2018**, *219*, 1800147.

(37) Ikeda, T. Preparation of (2×4)-Type Tetra-PEG Ion Gels through Cu-Free Azide-Alkyne Cycloaddition. *Polym. J.* **2020**, *52,* 1129−1135.

(38) Philp, D.; Slawin, A. M. Z.; Spencer, N.; Stoddart, J. F.; Williams, D. J. The Complexation of Tetrathiafulvalene by Cyclobis(paraquat-*p*-phenylene). *J. Chem. Soc., Chem. Commun.* **1991**, 1584−1586.

(39) Simonsen, K. B.; Zong, K. W.; Rogers, R. D.; Cava, M. P.; Becher, J. Stable Macrocyclic and Tethered Donor-Acceptor Systems. Intramolecular Bipyridinium and Tetrathiafulvalene Assemblies. *J. Org. Chem.* **1997**, *62,* 679−686.

(40) Flory, P. J. Molecular Theory of Rubber Elasticity. *Polym. J.* **1985**, *17,* 1−12.

(41) Flory, P. J. Network Structure and the Elastic Properties of Vulcanized Rubber. *Chem. Rev.* **1944**, *35,* 51−75.

(42) Billmeyer, F. W. Rheology and the Mechanical Properties of Polymers. In *Textbook of Polymer Science*, 3rd ed.; John Wiley & Sons, 1984; pp. 301−329.

(43) Hashimoto, K.; Fujii, K.; Nishi, K.; Sakai, T.; Shibayama, M. Nearly Ideal Polymer Network Ion Gel Prepared in pH-Buffering Ionic Liquid. *Macromolecules* **2016**, *49,* 344−352.

(44) Tsuji, Y.; Li, X.; Shibayama, M. Evaluation of Mesh Size in Model Polymer Networks Consisting of Tetra-Arm and Linear Poly(ethylene glycol)s. *Gels* **2018**, *4*, 50.

(45) Hunig, S.; Kiesslich, G.; Quast, H.; Scheutzow, D. Uber Zweistufige Redoxsysteme, X1) Tetrathio-Athylene Und Ihre Hoheren Oxidationsstufen. *Liebigs Ann. Chem.* **1973***,* 310−323.

(46) Schukat, G.; Fanghanel, E. Tetrathiafulvalene. XXII [1] Redox- Und Spektroskopische Eigenschaften Von Tetrathiafulvalenen (TTF) Und Tetraselenafulvalenen (TSF) Sowie Deren Mono- Und Dikationen. *J. Prakt. Chem.* **1985**, *327,* 767−774.

(47) Elofson, R. M.; Edsberg, R. L. Polarographic Behavior of the Viologen Indicators. *Can. J. Chem.* **1957**, *35,* 646−650.

(48) Bard, A. J.; Faulkner, L. R. Potential Sweep Methods. In *Electrochemical Methods: Fundamentals and Applications*, 2nd ed.; John Wiley & Sons, 2001; pp. 226−260.

(49) Tanaka, T.; Fillmore, D.; Sun, S. T.; Nishio, I.; Swislow, G.; Shah, A. Phase-Transitions in Ionic Gels. *Phys. Rev. Lett.* **1980**, *45,* 1636−1639.

(50) Torrance, J. B.; Scott, B. A.; Welber, B.; Kaufman, F. B.; Seiden, P. E. Optical-Properties of the Radical Cation Tetrathiafulvalenium ($TTF^{+}$) in Its Mixed-Valence and Mono-Valence Halide Salts. *Phys. Rev. B* **1979**, *19,* 730−741.

(51) Ziganshina, A. Y.; Ko, Y. H.; Jeon, W. S.; Kim, K. Stable π-Dimer of a Tetrathiafulvalene Cation Radical Encapsulated in the Cavity of Cucurbit[8]uril. *Chem. Commun.* **2004***,* 806−807.

(52) Spruell, J. M.; Coskun, A.; Friedman, D. C.; Forgan, R. S.; Sarjeant, A. A.; Trabolsi, A.; Fahrenbach, A. C.; Barin, G.; Paxton, W. F.; Dey, S. K.; Olson, M. A.; Benitez, D.; Tkatchouk, E.; Colvin, M. T.; Carmielli, R.; Caldwell, S. T.; Rosair, G. M.; Hewage, S. G.; Duclairoir, F.; Seymour, J. L.; Slawin, A. M. Z.; Goddard, W. A.; Wasielewski, M. R.; Cooke, G.; Stoddart, J. F. Highly Stable Tetrathiafulvalene Radical Dimers in [3]Catenanes. *Nat. Chem.* **2010**, *2,* 870−879.